

Targeting protein-protein interactions of tyrosine phosphatases with microarrayed fragment libraries displayed on phosphopeptide substrate scaffolds

Megan Hogan, Medhanit Bahta, Kohei Tsuji, Trung Xuan Nguyen, Scott Cherry, George T. Lountos, Joseph E. Tropea, Bryan Zhao, Xue Zhi Zhao, David S Waugh, Terrence R. Burke, and Robert G Ulrich

ACS Comb. Sci., **Just Accepted Manuscript** • DOI: 10.1021/acscmbosci.8b00122 • Publication Date (Web): 10 Jan 2019

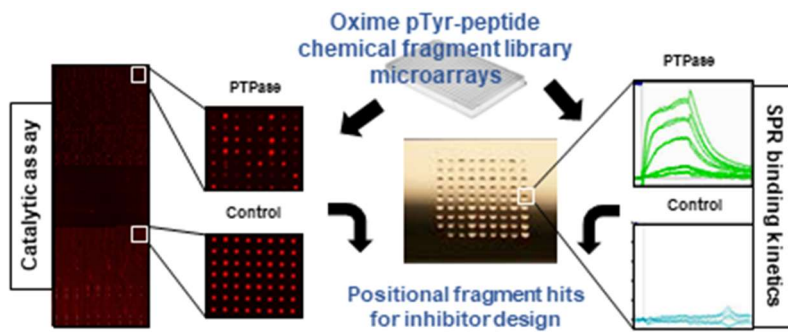
Downloaded from <http://pubs.acs.org> on January 16, 2019

Just Accepted

“Just Accepted” manuscripts have been peer-reviewed and accepted for publication. They are posted online prior to technical editing, formatting for publication and author proofing. The American Chemical Society provides “Just Accepted” as a service to the research community to expedite the dissemination of scientific material as soon as possible after acceptance. “Just Accepted” manuscripts appear in full in PDF format accompanied by an HTML abstract. “Just Accepted” manuscripts have been fully peer reviewed, but should not be considered the official version of record. They are citable by the Digital Object Identifier (DOI®). “Just Accepted” is an optional service offered to authors. Therefore, the “Just Accepted” Web site may not include all articles that will be published in the journal. After a manuscript is technically edited and formatted, it will be removed from the “Just Accepted” Web site and published as an ASAP article. Note that technical editing may introduce minor changes to the manuscript text and/or graphics which could affect content, and all legal disclaimers and ethical guidelines that apply to the journal pertain. ACS cannot be held responsible for errors or consequences arising from the use of information contained in these “Just Accepted” manuscripts.



Table of contents graphic



1
2
3
4
5
6
7
8
9
10
11
12
13
14
15
16
17
18
19
20
21
22
23
24
25
26
27
28
29
30
31
32
33
34
35
36
37
38
39
40
41
42
43
44
45
46
47
48
49
50
51
52
53
54
55
56
57
58
59
60

Targeting protein-protein interactions of tyrosine phosphatases with microarrayed fragment libraries displayed on phosphopeptide substrate scaffolds

Megan Hogan[†], Medhanit Bahta[‡], Kohei Tsuji[‡], Trung X. Nguyen[‡], Scott Cherry[§], George T. Lountos^{§,¥}, Joseph E. Tropea[§], Bryan M. Zhao[†], Xue Zhi Zhao[‡], David S. Waugh[§], Terrence R. Burke, Jr. [‡], Robert G. Ulrich^{†*}

[†]*Molecular and Translational Sciences Division, United States Army Medical Research Institute of Infectious Diseases, Frederick, MD 21702, USA;* [‡]*Chemical Biology Laboratory, Center for Cancer Research, National Institutes of Health, National Cancer Institute at Frederick, Frederick, Maryland 21702, United States;* [§]*Macromolecular Crystallography Laboratory, National Cancer Institute, National Cancer Institute at Frederick, Frederick, Maryland 21702, USA;* [¥]*Basic Science Program, Frederick National Laboratory for Cancer Research sponsored by the National Cancer Institute, Frederick, Maryland 21702, USA*

KEYWORDS

Aminoxy phosphopeptide, catalytic assay, fragment-based drug design, kinetic assay, microarray, oxime-containing phosphopeptide, protein tyrosine phosphatase, substrate affinity screening, surface plasmon resonance

ABSTRACT

Chemical library screening approaches that focus exclusively on catalytic events may overlook unique effects of protein-protein interactions that can be exploited for development of specific inhibitors. Phosphotyrosyl (pTyr) residues embedded in peptide motifs comprise minimal recognition elements that determine substrate specificity of protein tyrosine phosphatases (PTPases). Using solid-phase synthesis, we incorporated aminooxy-containing amino acid residues into a 7-residue epidermal growth factor receptor (EGFR)-derived phosphotyrosine-containing peptide and subjected the peptides to on-resin oxime diversification by reacting with aldehyde-bearing drug-like functionalities. The pTyr residue remained unmodified. The resulting derivatized peptide library was printed in microarrays on nitrocellulose-coated glass surfaces for assessment of PTPase catalytic activity, or on gold monolayers for analysis of kinetic interactions by surface plasmon resonance (SPR). Focusing on amino-acid positions and chemical features, we first analyzed dephosphorylation of the peptide pTyr residues within the microarrayed library by the human dual-specificity phosphatases (DUSP) 14 and DUSP22, as well as by PTPases from poxviruses (VH1) and *Yersinia pestis* (YopH). In order to identify the highest affinity oxime motifs, the binding interactions of the most active derivatized phosphopeptides were examined by SPR using noncatalytic PTPase mutants. Based on high-affinity oxime fragments identified by the two-step catalytic and SPR-based microarray screens, low molecular weight non-phosphate-containing peptides were designed to inhibit PTP catalysis at low micromolar concentrations.

INTRODUCTION

Protein tyrosine phosphatases (PTPases) dephosphorylate tyrosine residues within proteins and work in concert with protein tyrosine kinases to regulate signal transduction pathways. Because of the critical involvement of signal transduction pathways in regulating pathological processes in cancer and infectious diseases,¹⁻² PTPases have emerged as important targets for development of therapeutic inhibitors. Despite growing successes in the development of small molecules that inhibit kinases, modulators of PTPases have proven to be far more challenging, and no inhibitor has yet achieved clinical approval.³ Effective PTPase targeting by small molecule inhibitors is complicated by the relatively smooth protein surfaces and in the case of dual-specificity PTPases (DUSPs), shallow catalytic pockets that accommodate phosphotyrosine (pTyr), phosphoserine (pSer) and phosphothreonine (pThr) residues. In addition, because recognition and binding of PTPase substrates involves a network of hydrogen and ionic bonds within a highly conserved catalytic pocket [(H/V)C(X5)R(S/T)], preferred ligands are typically negatively-charged, which results in limited specificity, cell permeability and bioavailability. An alternative approach to increase the likelihood of finding druggable features of PTPases is to exploit interactions with protein features that extend beyond the catalytic pocket. Synthetic peptide substrates have previously been used as display platforms for non-hydrolyzable pTyr-mimicking residues,⁴ which led to the identification of the difluorophosphonomethyl-aryl moiety as a starting point for the design of small molecule inhibitors by converting a good substrate into a high affinity inhibitor.^{4,5} In the approach described herein, we used a high-affinity peptide substrate as a scaffold for presenting microarrayed libraries of drug-like fragments to identify motifs for inhibitor design.⁶⁻⁹ The goal of this work was to devise a method for developing inhibitors of protein-protein interactions (PPIs) that are intrinsic to PTPase catalytic specificities. In order to investigate substrate

1
2
3 binding interactions in proximity to the PTPase catalytic cleft, we sequentially examined
4 modified amino acid residues adjacent to the unaltered the pTyr residue of the peptide. A
5 diversified library was created by incorporating 300 different drug-like fragments at six
6 different positions on the EGFR-derived peptide, "VDADEpYL". Detailed interactions with
7 the substrate library were examined using PTPases from smallpox virus [Variola major H1
8 (VH1)], the plague bacillus [*Yersinia* outer protein H (YopH)], and the human enzymes
9 DUSP14 and DUSP22. In order to identify fragments that could be useful in inhibitor design,
10 primary results were obtained from catalytic assays with the microarrayed library, and kinetic
11 binding data were obtained from the microarrayed library by using a biosensor assay. As proof-
12 of-principal, a high-affinity oxime fragment identified by the two-step catalytic and SPR-based
13 microarray screens was employed to design low molecular weight, non-phosphate-containing
14 peptides, which were able to inhibit PTP catalysis at low micromolar concentrations.

31 RESULTS AND DISCUSSION

32
33 **Methodology.** A flowchart depicting the general approach used is presented in Figure 1. We
34 synthesized a library comprised of 1800 distinct oxime-modified phosphopeptides based on
35 the EGFR-derived heptapeptide sequence (biotin-linker-VDADEpYL-NH₂, **5**), which includes
36 the autophosphorylation site Tyr 992.¹⁰ The EGFR-derived pTyr-containing peptide is a
37 reliable substrate for many PTPases.¹¹⁻¹² Along with **5**, the library was deposited by inkjet
38 printing of microarrays on either a nitrocellulose-coated or a gold-coated glass slide for use in
39 a fluorescent-based catalytic assay or surface plasmon resonance (SPR) based kinetic assay,
40 respectively. The percent dephosphorylation (compared to the parent peptide **5**) and the binding
41 interaction of each library component with PTPases was assessed with VH1, DUSP14,
42 DUSP22) and YopH. Combining the data from both experiments allowed us to identify
43 fragments that may have the greatest utility as building blocks for design of potential inhibitors.

Active, wild-type PTPases were used for all catalytic assays, while catalytically inactive mutant enzymes were used in SPR binding-interaction studies to avoid dephosphorylation of the pTyr residue. These PTPase substrate-trapping mutants, which do not possess measurable catalytic activities but still bind tightly to pTyr-substrates,¹³ can be used to identify physiological substrates *in vivo* and *in vitro*,¹⁴ as well as to elucidate binding modes by crystallography.¹⁵

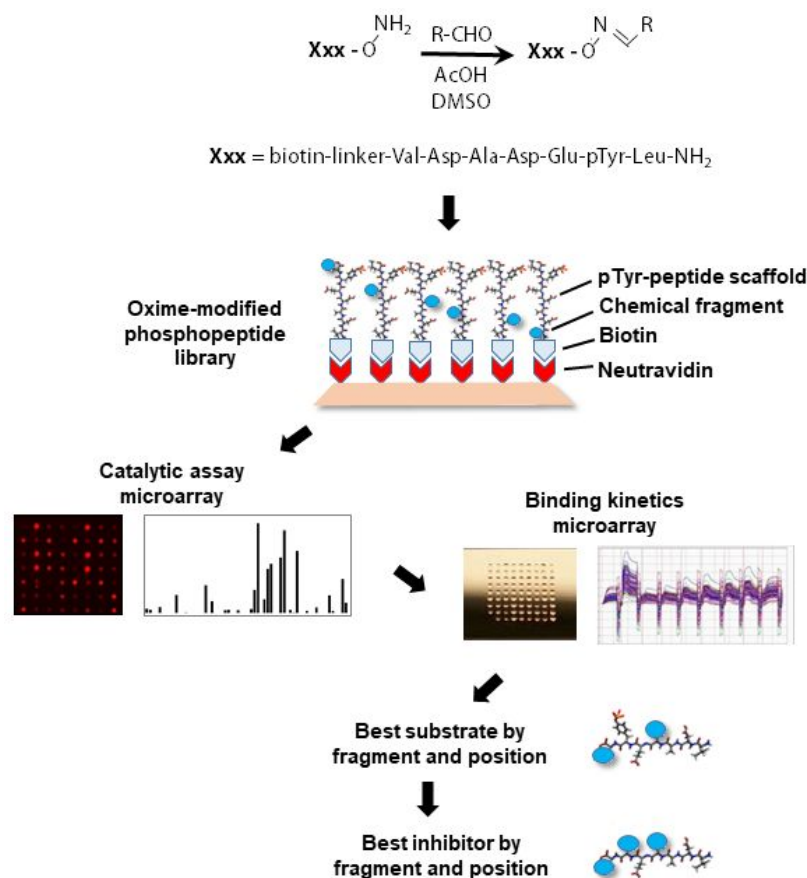
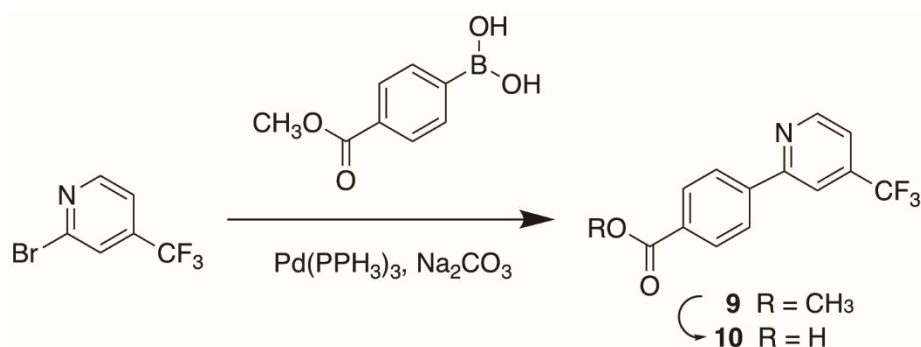


Figure 1. A flowchart depicting the methodology used in this study.

Synthetic Discussion

Synthesis of aminoxy-containing amino acid reagent 4. The preparation of aminoxy-containing peptides **6(a – f)** (Figure 2) by standard Fmoc-based solid-phase protocols entailed use of the orthogonally-protected amino acid **4** (Scheme 1). The synthesis of **4** started from compound **1**, which was obtained from Cbz-(Asp)-OBn by literature procedures.¹⁶ Reaction of

1
2
3 **1** with *N*-hydroxyphthalimide under Mitsunobu coupling conditions gave the adduct **2** in good
4 yield. Similar Mitsunobu coupling on the carboxymethyl ester variant of **1** had been reported
5 to give low yields and cyclized byproducts.¹⁷ This necessitated a two-step protocol that
6 involved conversion of the side chain hydroxyl to a mesyl ester followed by nucleophilic
7 displacement with *N*-hydroxyphthalimide.¹⁷ Starting from **1** a similar two-step approach has
8 been reported to prepare **2**.¹⁶ In the current work, treatment of **2** with methylhydrazine removed
9 the phthalimide group to provide the free aminoxy group, which was derivatized with Boc
10 anhydride to give the globally-protected analog **3** (Scheme 1). Hydrogenolytic removal of the
11 *N*-Cbz and *O*-Bn groups, followed by treatment with Fmoc succinimidyl carbonate (Fmoc-OSu)
12 and NaHCO₃ in aqueous dioxane, gave the desired *N*-Fmoc-protected **4** in good yield. The
13 synthesis of **4** has been previously reported by a slightly different protocol.¹⁷⁻¹⁸ Reagent **4** was
14 employed in solid-phase peptide synthesis (SPPS), using standard Fmoc procedures to prepare
15 the biotinylated aminoxy-containing peptides **6a** – **6f** (Figure 2).
16
17
18
19
20
21
22
23
24
25
26
27
28
29
30
31
32
33
34
35
36
37
38
39
40
41
42
43
44
45
46
47
48
49
50
51
52
53
54
55
56
57
58
59
60



Scheme 1. Synthesis of the orthogonally-protected amino acid reagent **4**.

- 5** Q-Val-Asp-Ala-Asp-Glu-pTyr-Leu-amide **6d** Q-Val-Asp-Ala-**Xxx**-Glu-pTyr-Leu-amide
6a Q-**Xxx**-Asp-Ala-Asp-Glu-pTyr-Leu-amide **6e** Q-Val-Asp-Ala-Asp-**Xxx**-pTyr-Leu-amide
6b Q-Val-**Xxx**-Ala-Asp-Glu-pTyr-Leu-amide **6f** Q-Val-Asp-Ala-Asp-Glu-pTyr-**Xxx**-amide
6c Q-Val-Asp-**Xxx**-Asp-Glu-pTyr-Leu-amide

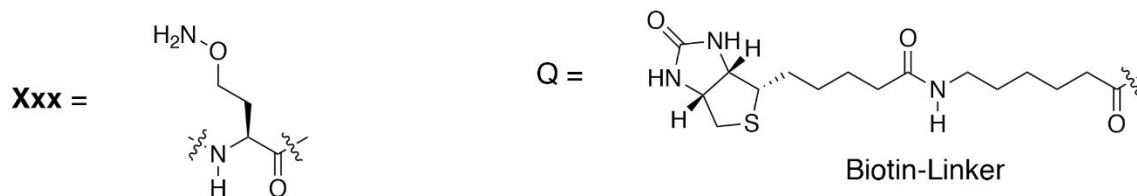
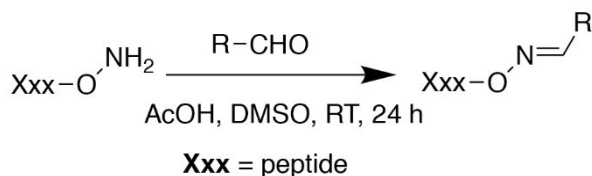


Figure 2. Structures of the parent peptide **5** and the biotinylated aminoxy-containing peptides **6(a-f)**.

Synthesis of a library of biotinylated oxime-containing peptides. Peptides and proteins undergo clean oxime-forming reactions rapidly and in near quantitative without the need of sidechain protection. The resulting products are highly stable.¹⁹⁻²¹ We have previously prepared libraries of oxime-diversified peptides by incorporating aminoxy-containing residues within parent peptides and then reacting the peptides in parallel with aldehydes in DMSO in the presence of acetic acid. The oxime-forming reactions were nearly quantitative and products of >90% purity were routinely obtained. These products are stable and can be subjected directly to biological evaluation without a need for purification.²²⁻²⁵ In our current work we employed a collection of 300 aldehydes (structures are shown in Supporting Information Tables S1 – S3) that were reacted with the biotinylated aminoxy-containing peptides **6a – 6f**. The optimized reaction conditions for oxime ligation used DMSO as solvent and acetic acid as catalyst at room temperature overnight, with molar concentrations of aminoxy: RCHO: acetic acid; 1:1:5 (Scheme 2).^{18, 19} This resulted in the formation of a library of 1800 distinct oxime-containing phosphopeptides at final concentrations of 100 μ M. In light of well-established precedence, the libraries were used without purification and the

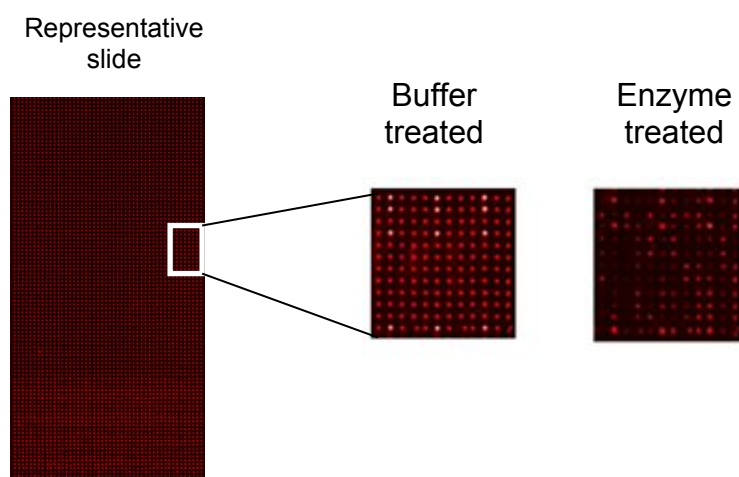
1
2
3 solutions were used directly to prepare microarrays on nitrocellulose slides²⁶ for screening as
4
5 described below.
6
7
8
9
10
11



19 **Scheme 2.** Synthesis of oxime-containing peptide library. The aldehydes are listed in
20
21 Supporting Information Tables S1 – S3.
22
23
24
25

26 **Synthesis of sidechain-modified peptides 11a,b and 12.** Oxime-containing peptides that
27
28 displayed the aldehydes **w33** and **w202** (Supporting Table S2, Supporting Figure S2) were
29
30 selected for further examination from the high-affinity substrates observed in the microarray
31
32 assays. The original oxime-aminoxy oxygens of **w33** and **w202** were replaced by methylene
33
34 groups, while the remainder of the oxime functionality was replaced by structurally
35
36 homologous amides. This resulted in the design of peptides **11a** (**w33**) and **11b** (**w202**) as the
37
38 monosubstituted congeners, and peptide **12** as a disubstituted congener that combined features
39
40 of peptides **w33** and **w202** (Figure 3). An essential feature of **11a,b** and **12** was the inclusion
41
42 of ornithine residues as homologous variants of the aminoxy-containing residue **4**. By
43
44 employing 4-methyltrityl (Mtt) sidechain amine protection of the ornithine residues in
45
46 combination with Rink amide MBHA resin, it was possible to remove the Mtt protection by
47
48 treatment with a low concentration of TFA (1%) that preserved peptide attachment to the resin.
49
50 Amidation of the ornithine sidechain was then achieved using the appropriate carboxylic acid
51
52 prior to Fmoc removal and peptide chain extension. Cleavage of the completed peptide from
53
54 the resin was then accomplished using 95% TFA. Although the 3,5-dichloropyridine-4-
55
56
57
58
59
60

1
2
3
4
5
6 **Fluorometric array.** The PTPase activity of each enzyme was measured against the peptide
7 libraries using a fluorescence-based microarray assay as a primary screening tool. The
8 unmodified EFGR-derived heptapeptide **5** served as a baseline to compare the effect of each
9 oxime-containing peptide within the library. The level of dephosphorylation was assessed by
10 using an antibody that detects phosphotyrosine within the substrate peptide and a fluorescently-
11 labeled secondary antibody (anti-mouse IgG). Figure 4 shows a representative slide of the
12 oxime-phosphopeptide library and controls that were spotted in triplicate and treated with
13 PTPase under fixed conditions. The magnified section compares the difference between a
14 buffer-treated slide (no PTPase) versus a PTPase-treated slide. Each spot represents an
15 individual phosphopeptide, and dephosphorylation is observed by a decrease in fluorescence
16 signal (Figure 4) as compared to the corresponding spot on the non-enzyme treated slide. The
17 results from each PTPase are depicted in the heat map diagram of Supplemental Figure S1,
18 which shows dephosphorylation values for individual components of the entire oxime-
19 containing phosphopeptide library, peptide **5**, and peptides **6(a – f)**.
20
21
22
23
24
25
26
27
28
29
30
31
32
33
34
35
36

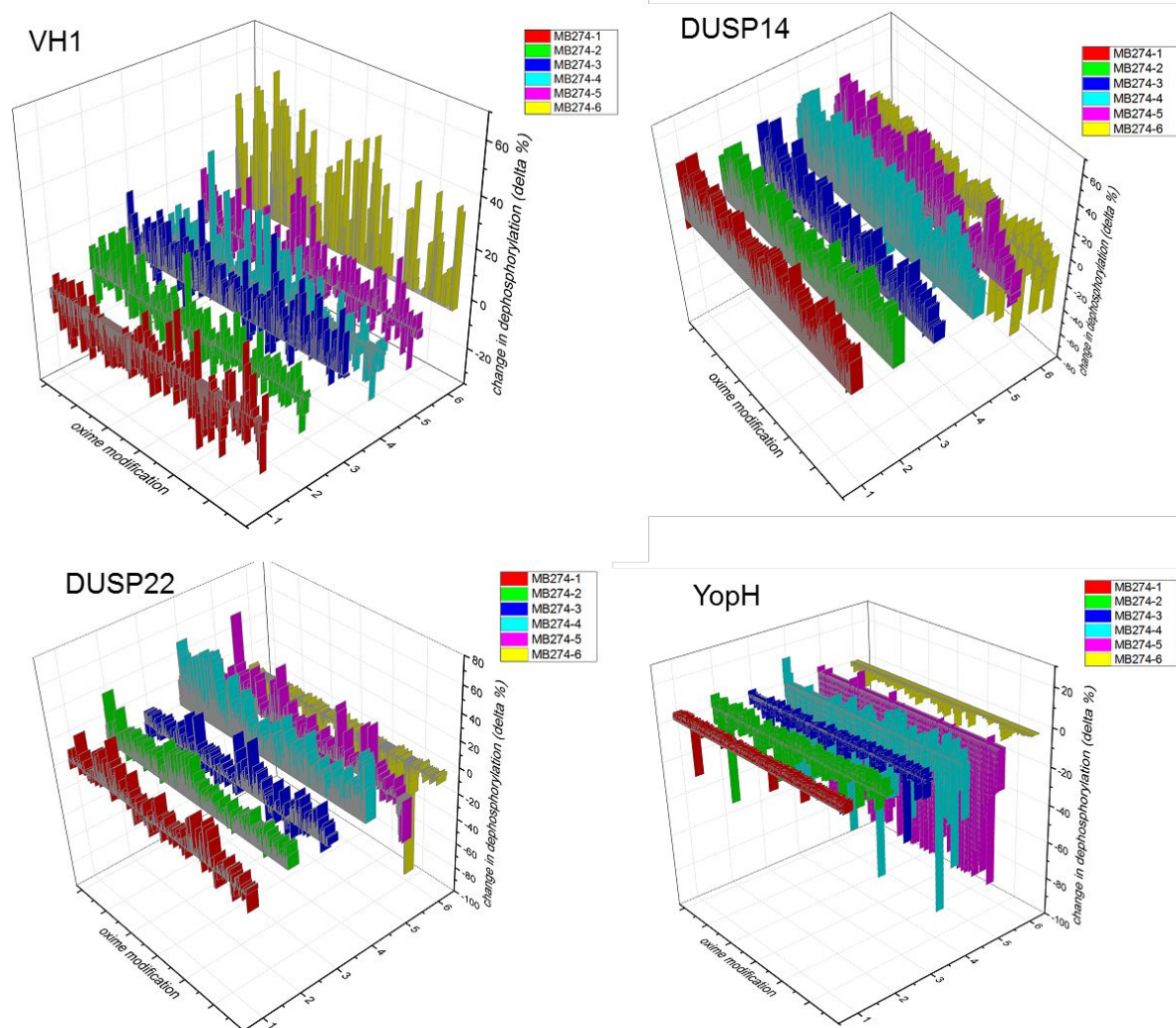


54 **Figure 4. A representative slide spotted with the oxime-containing phosphopeptide**
55 **library and treated with PTPase or buffer solution.** After probing with an
56 Alexafluor647®-conjugated detection antibody, the fluorescent signal from each spot is
57
58
59
60

1
2
3 measured. Strong signals are colored red and white and signify a greater amount of pTyr
4 remaining, while weaker signals are light red and black and signify less pTyr remaining. The
5
6 magnified images show the contrast between the buffer-treated and enzyme-treated slides.
7
8
9

10
11
12 Figure 5 shows the change in dephosphorylation for the oxime-containing phosphopeptides
13 when treated with each PTPase (averaged for each spot), as compared to **5** (the baseline). The
14 peptides are grouped according to the position of each amino-acid residue relative to pTyr.
15
16 Protein concentrations and incubation times were determined from test experiments of the
17 PTPases with **5** and **6(a – f)**, in which approximately 40% dephosphorylation was obtained
18 (data not shown). This was done in order to ascertain whether fragments particular to individual
19 oxime-containing peptides enhanced or reduced the dephosphorylation of pTyr residues in
20 comparison to the parent peptide **5**. When tested against the entire peptide library, the PTPase
21 activities of each enzyme with peptide **5** as substrate were as follows: VH1: 24%, DUSP14:
22 28%, DUSP22: 6%, YopH: 96%. This apparent change in dephosphorylation may be a result
23 of scaling up enzyme solutions for the larger peptide library, slight errors in measuring enzyme
24 concentration (by UV/Vis), and/or changes in the specific activity of the enzyme over time.
25
26 Because we were primarily interested in fragments associated with enhancing
27 dephosphorylation for use in the design of inhibitors, the dephosphorylation levels
28 corresponding to peptide **5** against VH1, DUSP14, and DUSP22 were acceptable. Although
29 the high activity of YopH across the entire library was not unexpected,²⁷ this made it difficult
30 to control cleavage conditions for YopH in this assay. As seen in figure 5, large differences
31 from the baseline (peptide **5**) for YopH are generally only apparent for decreases in percent
32 dephosphorylation. This inhibitory effect is most notable with the oxime-containing peptides
33 from **6d** and **6e**, in which the respective Asp and Glu residues have been modified. This is
34 consistent with findings from other studies showing that these two residues are crucial for
35
36
37
38
39
40
41
42
43
44
45
46
47
48
49
50
51
52
53
54
55
56
57
58
59
60

1
2
3 substrate-enzyme binding interactions.²⁸ The data set for YopH remains biased towards
4
5 decreases in dephosphorylation, due to the high amount of dephosphorylation observed with
6
7 the parent peptide **5**. For this reason, YopH was used as a positive control in subsequent binding
8
9 experiments and analyses. In Figure 5, VH1 demonstrates varying degrees of activity towards
10
11 the entire peptide library, with the exception of those in group **6f**, in which the Leu residue C-
12
13 proximal to the pTyr was modified.
14
15
16
17



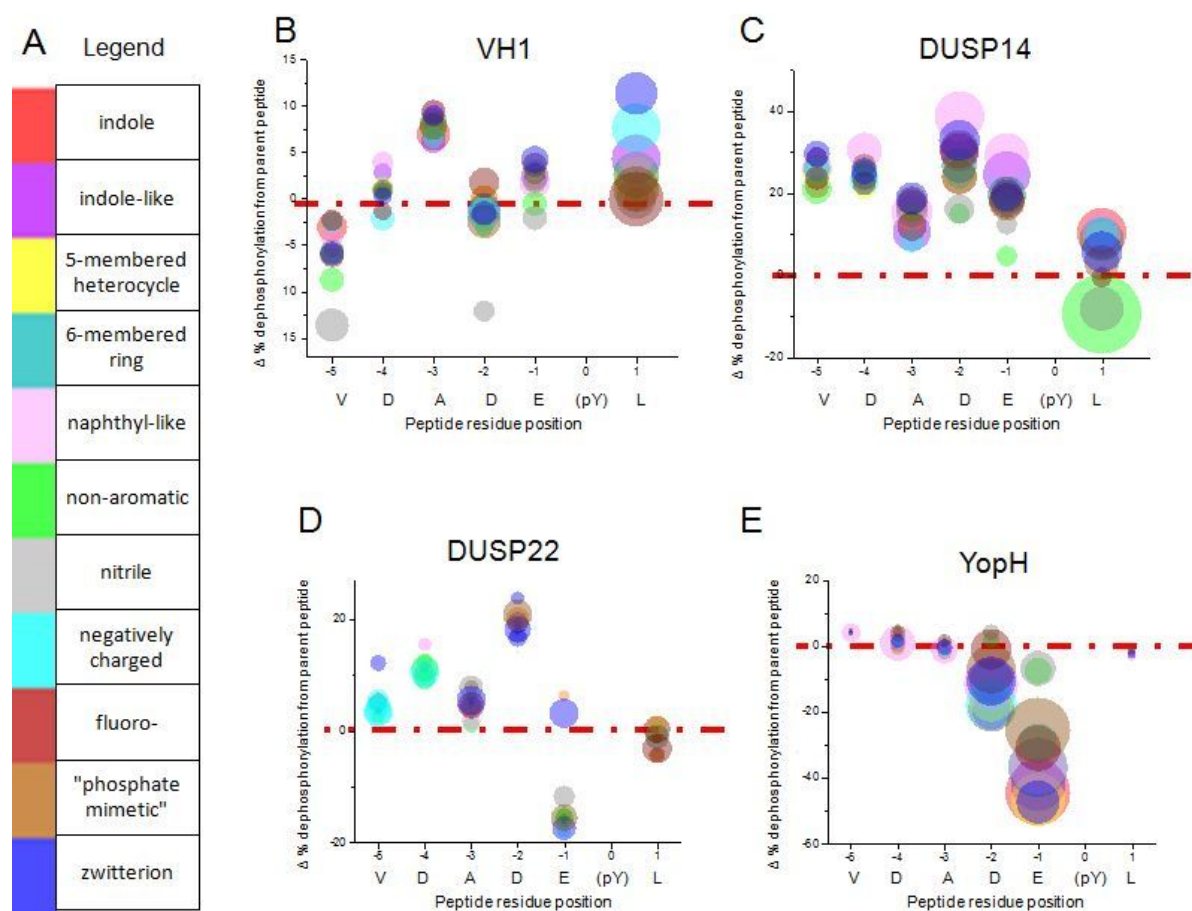
18
19
20
21
22
23
24
25
26
27
28
29
30
31
32
33
34
35
36
37
38
39
40
41
42
43
44
45
46
47
48
49
50
51 **Figure 5. The effect of residue position of the peptide on enzymatic cleavage of pTyr.**

52
53 The change in percent dephosphorylation as compared to parent peptide **5** for each oxime-
54
55 containing peptide, grouped according to the amino-acid residue that was modified **6(a – f)**.
56
57
58
59
60

1
2
3 Most of the peptides in **6f** appear to have an enhancing effect on VH1 PTPase activity. From a
4 drug design viewpoint, it may be advantageous to target areas on the protein that are reachable
5 from this residue, keeping in mind the more polar oxime-handle that replaced the bulkier alkyl
6 chain of the Leu. In contrast, DUSP14 appears to be less sensitive to residue positioning, with
7 the exception of the C-terminal Leu, as seen in Figure 5. Nearly all modifications to residues
8 in the N-terminal direction of pTyr produce an increase in dephosphorylation. Modification of
9 either of the Asp residues (groups **6b** or **6d**) appears to enhance DUSP22 activity (Figure 5),
10 indicating that negative chemical functionalities are disfavored at these positions for this
11 PTPase.
12
13
14
15
16
17
18
19
20
21
22
23

24 The fragments for each oxime-containing phosphopeptide were grouped into 11
25 categories according to chemical structure and functional group. For each of the 11 structural
26 categories, the median difference in percent dephosphorylation between each oxime-
27 phosphopeptide and **5** are depicted graphically in Figure 6. Differences in the abilities of the
28 functional groups to affect the PTPase dephosphorylation of the pTyr-containing peptides are
29 readily apparent. For clarity, the effects of each fragment have also been arranged according to
30 residue proximity to the pTyr residue and by PTPase. Bubble sizes represent the standard
31 deviations of the difference in percent dephosphorylation for the fragment-containing peptides
32 associated with that category (i.e., a smaller bubble signifies a tighter agreement between the
33 fragments in that category). The red dotted lines intersect the x-axis at zero to better visualize
34 effects that groups have on the ability of the PTPase to dephosphorylate the phosphopeptide
35 (bubbles above the line signify a median increase in percent dephosphorylation when compared
36 to **5**, while bubbles below the line signify a median decrease within the group). Because the
37 fragment library was chosen based on drug-like properties, many of the members possess
38 qualities of multiple functional/structural groups. Therefore, a high degree of overlap is not
39 surprising. However, a number of notable features can be discerned from these graphs. For
40
41
42
43
44
45
46
47
48
49
50
51
52
53
54
55
56
57
58
59
60

example, in the case of VH1 (Figure 6B), fragments containing nitrile groups seem to be particularly disfavored at the Val (-5) and Asp (-2) positions. Based on these results, it would be beneficial to avoid nitrile groups when designing VH1 inhibitors, at least in the chemical space associated with the areas on the protein that interact with these Val and Asp residues. In addition, although there is a high degree of overlap among many of the bubbles in the graph for DUSP22 (Figure 6D), there is a clear differentiation between the phosphate-mimetics and zwitterions versus the remaining groups at the Glu (-1) position. When designing inhibitors of DUSP22, it may be beneficial to place functional groups that possess phosphate-like qualities in close proximity. The large differences observed between each PTPase suggest that the enzymes may be selectively targeted using specifically designed small-molecules and the results could serve as a baseline for further structure-activity relationship studies.

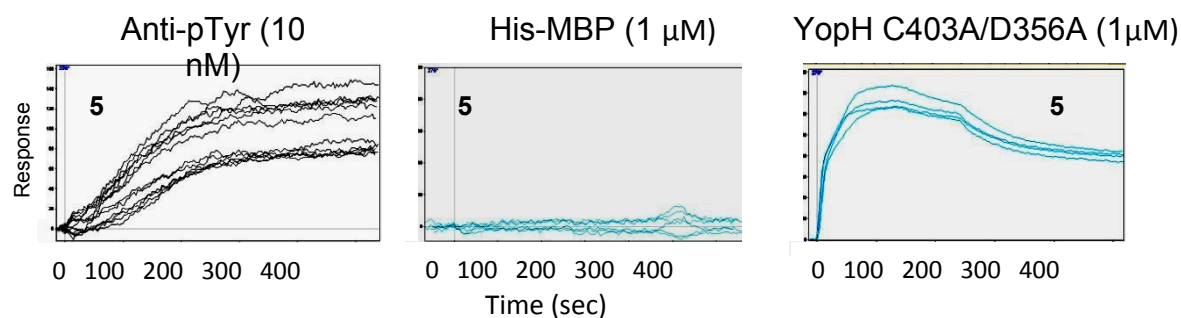


1
2
3 **Figure 6. The effect of functional group/chemical structure on enzymatic cleavage of**
4 **pTyr.** The change in percent dephosphorylation as compared to parent peptide **5** for each
5 oxime-containing peptide, grouped according to functional group/chemical structure as
6 named in the legend.
7
8
9
10

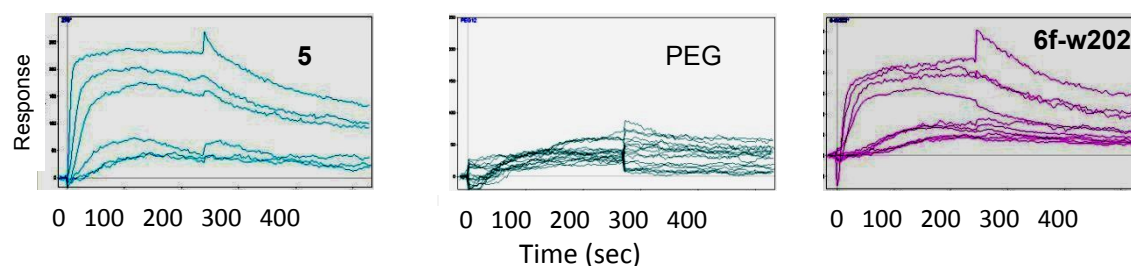
11
12
13
14 **PTPase kinetic interactions.** The binding interactions between a select number of oxime-
15 containing phosphopeptides and PTPases were calculated using an SPR-based biosensor that
16 permitted continuous measurement in real-time. For these kinetic assays, a subset of peptides
17 was chosen according to their range of activities observed in the catalytic assay. A total of 45
18 oxime-containing phosphopeptides were selected in order to accommodate controls and allow
19 for replicate spots. The chosen peptides include six that showed little to no dephosphorylation;
20 five peptides that showed specific activity towards a particular enzyme and 17 peptides that
21 showed the highest levels of dephosphorylation (representing at least one peptide from each of
22 the **6(a-f)** groups so that each residue position was included). The biotinylated-peptides and
23 controls were mixed with NeutrAvidin and each mixture was spotted onto a gold-coated SPR
24 slide that was derivatized with a self-assembled monolayer of carboxyl-terminated alkane
25 thiols followed by 1-ethyl-3-(3-dimethylaminopropyl)-carbodiimide (EDC)/*N*-
26 hydroxysuccinimide (NHS) coupling chemistry. Kinetic binding studies were then performed
27 for each PTPase, with anti-pTyr antibody and histidine-tagged maltose binding protein (His-
28 MBP) acting as positive and negative binding controls, respectively. Figure 7 shows
29 representative sensorgrams from the kinetic assays for the control proteins, VH1 C110S, and
30 DUSP14 C111S. For binding interactions between peptide **5** and the positive control proteins,
31 anti-pTyr mouse antibody and YopH, noticeable binding curves were observed, although the
32 slope of each curve was different. The on-rate (k_a) and off-rate (k_d) for the antibody were slower
33 than for YopH, indicating a slower but stronger complex formation. The binding curves
34
35
36
37
38
39
40
41
42
43
44
45
46
47
48
49
50
51
52
53
54
55
56
57
58
59
60

1
2
3 between VH1 C110S and peptides **5** and **6f-w202** (nomenclature indicates the parent peptide
4 with the associated oxime group as shown in Supporting Information Tables S1 – S3) as well
5 as the negative control, **PEG** [a 12-chain poly-(ethylene glycol) (PEG) with a terminal
6 ethanolamide] are shown in Figure 7B. As depicted, negligible binding was observed between
7 the PTPase and **PEG**, indicating little non-specific binding. The higher binding affinity for
8 VH1 and peptide **6f-w202** ($K_D = 73 (\pm 27)$ nM) versus peptide **5** ($K_D = 96 (\pm 21)$ nM) was
9 consistent with the higher level of dephosphorylation in the catalytic assay (43% and 24% for
10 peptides **6f-w202** and **5**, respectively). Binding curves for DUSP14 C111S and peptides **5**, **6f-**
11 **w99**, and **6f-w202** are shown in Figure 7C, with the associated K_D values for each peptide being
12 as follows: **5**, 1.4 ± 1.3 μ M; **6f-w202**, 642 ± 147 nM and **6f-w99**, 94 ± 94 nM. Binding curves
13 for **5** and **6f-w99** are atypical and probably are not best fit to a Langmuir binding curve (also
14 demonstrated by the high standard deviation values for both). However, the trend in measured
15 binding affinities are consistent with data from the corresponding catalytic assays, in which
16 dephosphorylation values of 28%, 87%, and 99% were observed, respectively. The high
17 binding affinity, and likely also the potency, of peptide **6f-w99** can be attributed to the slow
18 dissociation rate, which indicates a stable complex with the PTPase. Under the conditions used
19 for the other PTPases, binding interactions were not observed between DUSP22 and the
20 phosphopeptides, including the unmodified parent peptide. Figure 8 presents the kinetic data,
21 k_a (association rate or on-rate) and k_d (dissociation or off-rate), as it relates to the catalytic data
22 (percent dephosphorylation), for VH1 and DUSP14 with a subset of the oxime-containing
23 phosphopeptide library. From a drug design perspective, peptides that reside at the top of the
24 graph in the upper and lower left quadrants include fragments with ideal inhibitor qualities of
25 high catalytic activity and a long residence time (slow off-rate).
26
27
28
29
30
31
32
33
34
35
36
37
38
39
40
41
42
43
44
45
46
47
48
49
50
51
52
53
54
55
56
57
58
59
60

A Controls



B VH1 C110S



C DUSP14 C111S

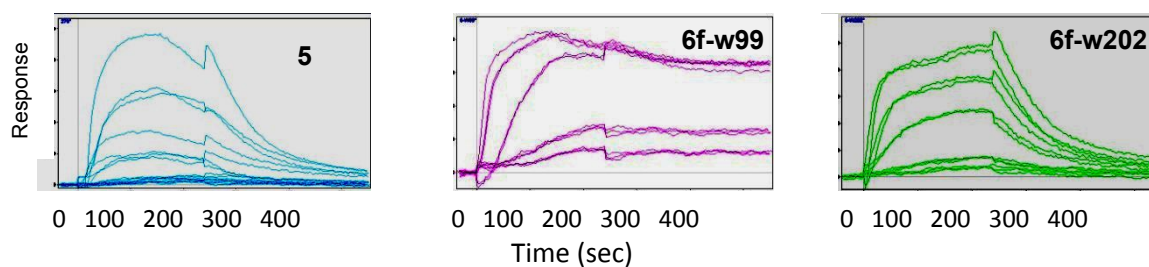


Figure 7. Biomolecular interactions of phosphatases and phosphopeptide substrates.

Representative sensorgrams depicting the kinetic interaction between each PTPase or control protein and the parent peptide **5**, negative control **PEG**, or oxime-containing peptide **6f-w202** and **6f-w99**.

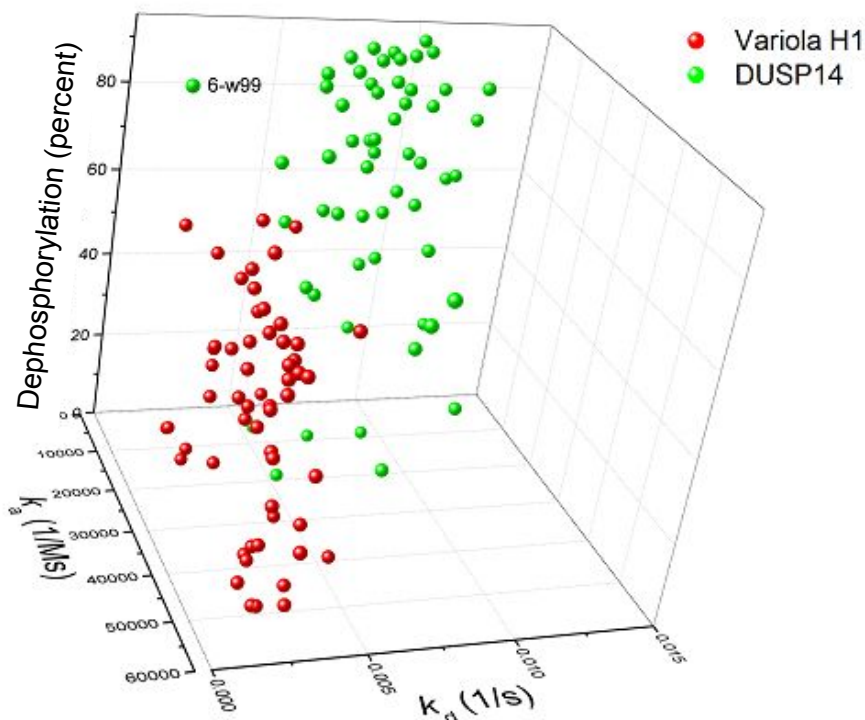
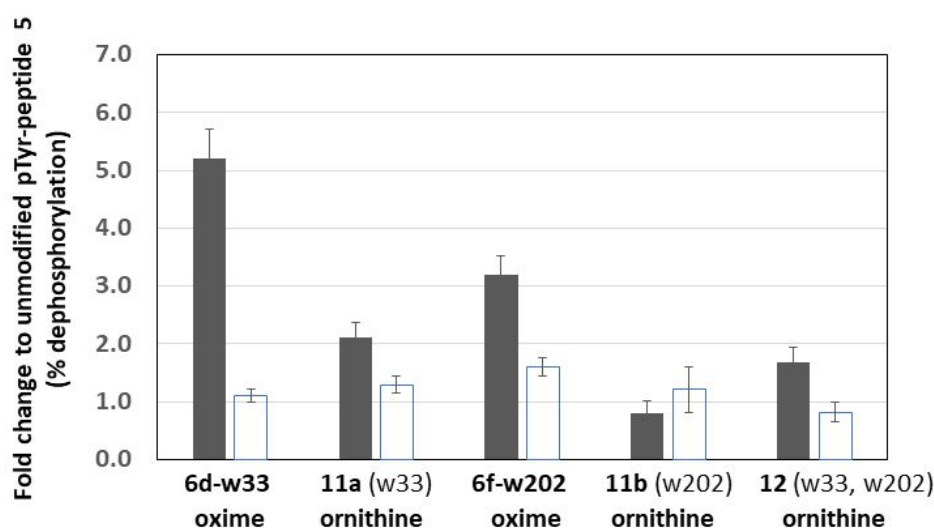


Figure 8. Depiction of catalytic and kinetic affinity. Mapping the on-rate (k_a) and off-rate (k_d) of each ligand-enzyme interaction with respect to catalytic activity (% dephosphorylation). Labels are included for select oxime-containing peptides.

Substrate enhancement and PTPase inhibitors. Peptide **12** was synthesized in order to test whether multiple fragments that increased dephosphorylation and binding activity (as compared to **5**) could be combined to generate an additive effect (Figure 3). Using ornithine amides to stabilize the fragment bonds, peptide **12** merges two fragments (**w33** and **w202**) that showed moderate-to-high affinity for VH1 and DUSP14 in both assays. The dually-functionalized phosphopeptide **12** was spotted onto a nitrocellulose slide, along with the mono-substituted peptides (**11a** and **11b**), the original oxime-containing phosphopeptides **6d-w33** and **6f-w202**, and the parent peptide **5**. The catalytic assay was performed in the same manner as with the oxime-containing library described previously. The percent dephosphorylation

1
2
3 results are presented in Figure 9 as fold-change relative to the percent dephosphorylation of **5**.
4
5 Peptides modified with 4-(4-(trifluoromethyl)pyridin-2-yl) benzoic acid (**w33**) presented the
6
7 highest activities, especially with VH1, while the ornithine amides reduced substrate activity
8
9 levels. However, there was no clear enhancement of catalytic activity towards the bisubstituted
10
11 peptide in comparison with the monosubstituted peptide. Though not further tested, it is
12
13 conceivable that other fragment combinations besides **w33** and **w202** may result in increased
14
15 PTPase activity. Since the fragment motifs were envisioned to afford enhanced interactions
16
17 with regions proximal to but outside the catalytic cleft, we wondered whether reasonable
18
19 affinity could be retained in the absence of the pTyr residue. In order to examine this hypothesis,
20
21 peptides **13** – **15** were synthesized (Scheme 4) by tethering two **w33** fragments in
22
23
24
25
26
27
28



29
30
31
32
33
34
35
36
37
38
39
40
41
42
43
44
45
46
47
48
49
50
51
52
53
54
55
56
57
58
59
60
Figure 9. Enhanced peptide substrates. Peptides substituted with fragments **w33** and **w202** were examined as oxime or ornithine amides in a PTPase assay with VH1 (dark bars) and DUSP14 (open bars). Fragments **w33** and **w202** merged onto a single peptide backbone (**12**) were compared to mono-substituted peptides (**11a, b**). Data \pm SD are presented as substrate activity (fold change) compared to the unmodified peptide **5**.

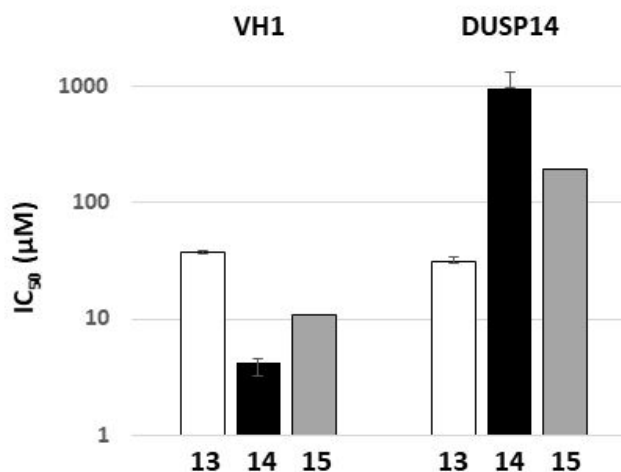


Figure 10. Transformation of high affinity substrates to inhibitors by substitution of two fragments onto a single peptide scaffold. Side chains of peptides **13**, **14**, and **15** were replaced with a hydrolytically-stable mimic of the oxime group from **6d-w33** and tested in a PTPase assay with peptide **5** as the substrate. Potencies for inhibition of peptide **5** dephosphorylation ($IC_{50} \pm SD$) are shown.

CONCLUSION

Combinatorial synthetic efforts that targeted key substrate interactions with the catalytic site were previously reported to develop potent PTPase inhibitors^{29,30}. In the study described here, diverse chemical fragments were introduced into all residues of a short peptide substrate as the basis of a combinatorial screening approach. We synthesized a tethered fragment library of 1800 unique oxime phosphopeptide derivatives of a high affinity heptapeptide scaffold that is widely employed as a general PTPase substrate. The entire oxime-containing peptide library was spotted onto microarray slides and evaluated against a panel of PTPases. This allowed us to measure a total of 7200 different catalytic interactions in a single assay. The results were analyzed according to amino acid position on the peptide chain, as well as by chemical structure or functional group of each oxime-derived fragment. The potencies of select oxime-containing

1
2
3 peptides were confirmed by a microarray-based kinetic assay that simultaneously measured the
4 association and dissociation rates of up to 200 peptide-enzyme complexes in real-time. By
5
6 combining the results from the catalytic and the kinetic assays, we identified multiple
7
8 fragments that were preferred in different locations on the peptide. We removed the pTyr
9
10 residue to form tethered bivalent constructs **13** – **15** and found that these exhibited micromolar
11
12 PTPase inhibitory potencies. We rationalized that this reflected enhanced non-pTyr-dependent
13
14 interactions with regions proximal to, but outside, the catalytic cleft. Collectively, these results
15
16 suggest that chemical fragments identified by the described peptide-display method can be used
17
18 as building blocks for designing non-peptidyl inhibitors of PTPases.
19
20
21
22
23
24
25

26 **EXPERIMENTAL SECTION**

27 28 29 **Synthetic**

30
31
32
33 **General.** The following reagents are commercially available from Sigma–Aldrich: 2-bromo-
34 4-(trifluoromethyl)pyridine (**7**) (cat. no. 661139); 4-(methoxycarbonyl)phenylboronic acid (**8**)
35 (cat. no. 594539). The following reagents are available from Chem–Impex, International:
36 Fmoc-Orn(Mtt)-OH (cat. no. 03729); Fmoc-L-Tyr(HPO₃Bzl)-OH (cat. no. 03746); Fmoc-
37 Glu(O^tBu)-OH (cat. no. 02413); Fmoc-Asp(O^tBu)-OH (cat. no. 00494); Fmoc-Ala-OH (cat.
38 no. 02369); Fmoc-Val-OH (cat. no. 02470) and (+) biotinyl-6-aminohexanoic acid (cat. no.
39 14003). Preparative high-pressure liquid chromatography (HPLC) was conducted using a
40 Waters Prep LC4000 system having photodiode array detection and Phenomenex C₁₈ columns
41 (250 mm × 21.2 mm, 10 μm particle size, 110 Å pore size) at a flow rate of 10 mL/min. Binary
42 solvent systems were employed consisting of A = 0.1% aqueous TFA and B = 0.1% TFA in
43 CH₃CN. Purified samples were lyophilized to provide final products as white powders. The
44 mass spectra of final peptides were measured by electrospray ionization-mass spectra (ESI-MS)
45
46
47
48
49
50
51
52
53
54
55
56
57
58
59
60

1
2
3 using an Agilent 1200 HPLC system equipped with a diode-array detector set to measure UV
4 absorption at 220 nm. Chromatography was carried out on a narrow-bore (100 mm × 2.1 mm),
5 small-particle (3.5- μ m), Zorbax Rapid-Resolution reversed-phase C₁₈ column coupled with a
6 C₁₈ guard column of the same bonded phase (12.5 mm × 2.1 mm) eluted with a linear gradient
7 of MeOH : H₂O at a flow rate of 300 μ L/min. Solvent A consisted of 5% CH₃OH/H₂O
8 containing 0.1% CH₃COOH and solvent B consisted of 90% CH₃OH/H₂O containing 0.1%
9 CH₃COOH was employed in the following gradient: isocratic A for 3 min; linear gradient of B
10 to 100% B in 9 min; isocratic B for 5 min; linear reset to 100 % A in 5 min; isocratic A for 3
11 min to equilibrate.
12
13
14
15
16
17
18
19
20
21
22
23
24
25

26 **Synthesis of (S)-benzyl-2-(((benzyloxy)carbonyl)amino)-4-(((tert-**
27 **butoxycarbonyl)amino)oxy)butanoate (3).**
28
29

30 To a solution of **2** (2.96 g, 6.1 mmol) in CH₂Cl₂ (10 mL) at 0 °C was added methyl hydrazine
31 (0.80 mL, 0.70 mmol) and the reaction mixture was stirred at 0 °C (2 h). The mixture was
32 filtered and the filtrate was concentrated and dried under high vacuum. The resulting crude
33 material was dissolved in THF (10 mL) and to this was added triethylamine (1.22 mL, 0.89
34 mmol) and Boc₂O (1.9 g, 1.9 mmol) and the solution was stirred at room temperature
35 (overnight). The reaction mixture was diluted with EtOAc (20 mL) and washed with H₂O (2 ×
36 20 mL) and brine (20 mL) and dried (MgSO₄). The crude material was purified using silica gel
37 CombiFlash (Hex : EtOAc, 2 : 1) to give product **3** as a colorless oil (1.86 g, 4.1 mmol, 72 %).
38
39
40
41
42
43
44
45
46
47
48
49 ¹H NMR (400 MHz, CDCl₃) δ 7.23-7.31 (m, 10H), 5.12 (m, 2H), 5.08 (m, 2H), 4.52 (m, 1H),
50 3.81-3.92 (m, 2H), 2.09 (m, 2H), 1.42 (s, 9H). ¹³C NMR (400 MHz, CDCl₃) δ 171.87 (1C),
51 156.89 (1C), 156.14 (1C), 136.36 (1C), 135.27 (1C), 128.52 (2C), 128.40 (2C), 128.35 (1C),
52 128.24 (2C), 127.97 (1C), 127.85 (2C), 85.10 (1C), 72.76 (1C), 67.17 (1C), 66.78 (1C), 51.72
53
54
55
56
57
58
59
60

1
2
3 (1C), 30.25 (1C), 28.11 (3C). ESI -MS (m/z): Calcd. for $C_{24}H_{30}N_2O_7 + Na$, 481.2; Found, 481.2
4
5 [M + Na]⁺.
6
7
8
9

10
11 **(S)-2-(((9H-fluoren-9-yl)methoxy)carbonyl)amino)-4-(((tert-**
12
13 **butoxycarbonyl)amino)oxy)butanoic acid (4).**

14 A mixture of **3** (1.86 g, 4.1 mmol) and 10% Pd•C (0.19 g) was dissolved in MeOH (5 mL) and
15 stirred under H₂ (overnight). The mixture was passed through Celite and the solvent was
16 removed under reduced pressure. The crude material was dissolved in dioxane (10 mL) and
17 H₂O (10 mL) and FmocOSu (1.64 g, 8.2 mmol) and NaHCO₃ (0.68 g, 4.9 mmol) were added
18 and the reaction mixture was stirred at room temperature (overnight). The reaction mixture was
19 washed with Et₂O (10 mL) and the remaining aqueous layer was acidified with 1N HCl to pH
20 3 – 4 and extracted with EtOAc (3 x 20 mL). The organic phase was dried (MgSO₄), filtered
21 and the was solvent evaporated. The crude product was purified using silica gel CombiFlash
22 (MeOH/CH₂Cl₂ 0-85%) and lyophilized from CH₃CN : H₂O (1 : 1 with 0.1%TFA) to provide
23 product **4** as a white solid (1.65 g, 3.6 mmol, 88 %). ¹H NMR (400 MHz, CDCl₃) δ 7.72 (d, J
24 = 7.2 Hz, 2H), 7.62 (d, J = 7.2 Hz, 2H), 7.41 (s, 1H), 7.36 (t, J = 7.2 Hz, 2H), 7.27 (td, J = 1.2,
25 7.2 Hz, 2H), 4.57 (m, 1H), 4.36 (m, 2H), 4.21 (m, 1H), 3.96 (m, 1H), 2.14 (m, 1H), 1.46 (s,
26 9H). ¹³C NMR (400 MHz, CDCl₃) δ 174.86 (1C), 157.78 (1C), 156.69 (1C), 143.87 (1C),
27 143.73 (1C), 141.23 (2C), 127.64 (2C), 127.04 (1C), 127.02 (1C), 125.22 (2C), 119.88 (2C),
28 82.71 (1C), 73.24 (1C), 67.26 (1C), 51.79 (1C), 47.08 (1C), 29.85 (1C), 28.11 (3C). ESI -MS
29 (m/z): Calcd. for $C_{24}H_{28}N_2O_7 + Na$, 479.2; Found, 479.2 [M + Na]⁺.
30
31
32
33
34
35
36
37
38
39
40
41
42
43
44
45
46
47
48
49
50
51
52
53

54 **Methyl 4-(4-(trifluoromethyl)pyridin-2-yl)benzoate (9).** To a solution of 2-bromo-4-
55 (trifluoromethyl)pyridine (**7**) (0.547 mL, 4.42 mmol) in a solution of toluene : EtOH : H₂O (5 :
56 1 : 5, 26.4 mL) was added Na₂CO₃ (4.22 g, 39.8 mmol), Pd(PPh₃)₄ (0.511 g, 0.442 mmol) and
57
58
59
60

1
2
3 (4-(methoxycarbonyl)phenyl)boronic acid (**8**) (1.194 g, 6.64 mmol) and the mixture was stirred
4
5 at 110 °C (overnight). The mixture was cooled to room temperature, diluted with EtOAc (200
6
7 mL) and washed with H₂O (50 mL) and brine (2 × 50 mL) then dried (Na₂SO₄), filtered and
8
9 concentrated. The resulting residue was purified by silica gel CombiFlash to provide **9** as a
10
11 white solid (805 mg, 65 % yield). ¹H NMR (400 MHz, CDCl₃) δ 8.83 (d, *J* = 5.0 Hz, 1H), 8.11
12
13 (d, *J* = 8.4 Hz, 2H), 8.05 (d, *J* = 8.4 Hz, 2H), 7.91 (d, *J* = 0.6 Hz, 1H), 7.46-7.41 (m, 1H), 3.90
14
15 (s, 3H). DUIS-MS *m/z*: 282 (MH⁺).
16
17
18
19
20

21
22 **4-(4-(Trifluoromethyl)pyridin-2-yl)benzoic acid (10)**. To a solution of **9** (805 mg, 2.86 mmol)
23
24 in THF : H₂O (2 : 1, 9 mL) was added LiOH·H₂O (240 mg, 5.7 mmol) and the mixture was
25
26 stirred at room temperature (overnight). The mixture was acidified with ethereal HCl (3 mL,
27
28 2.0 M in Et₂O) and concentrated and the resulting residue was suspended in MeOH (3 mL),
29
30 collected by filtration, washed (MeOH) and dried to provide **10** as a white solid (757 mg, 99
31
32 % yield). ¹H NMR (400 MHz, DMSO-*d*₆) δ 13.04 (brs, 1H), 8.93 (d, *J* = 5.0 Hz, 1H), 8.34 (s,
33
34 1H), 8.31-8.22 (m, 2H), 8.03 (dd, *J* = 8.2, 1.3 Hz, 2H), 7.74 (d, *J* = 5.0 Hz, 1H). ESI-MS *m/z*:
35
36 268.1 (MH⁺).
37
38
39
40
41

42 **Synthesis of peptides 5 and 6(a – f)**. Peptides were synthesized on Rink amide MBHA resin
43
44 (Novabiochem, cat. no. 01-64-0037) by standard Fmoc solid-phase protocols using active ester
45
46 coupling methodology in *N,N*-dimethylformamide (DMF). In summary, coupling was achieved
47
48 by reacting each residue, amino acid or acid (5.0 equivalents based on resin loading), 1-
49
50 hydroxybenzotriazole (HOBt) (5.0 eq.) and *N,N'*-diisopropylcarbodiimide (DIC) (5.0 eq.)
51
52 (single couple, 2 h). Peptides **6(a – f)** were prepared using reagent **4** where appropriate. The
53
54 final resin was washed with DMF, MeOH, CH₂Cl₂, and Et₂O and then dried under vacuum
55
56 (overnight). Peptides were cleaved from the resin by treatment with TFA : triisopropylsilane
57
58
59
60

(TIPS)/H₂O (95: 2.5: 2.5, 5 mL, 4 h). The resin was removed by filtration, the peptide was precipitated in cold Et₂O and the precipitate was centrifuged and washed with Et₂O. The resulting white solid was dissolved in 50% aqueous CH₃CN (4 mL) and purified by reverse phase preparative HPLC. (Analytical HPLCs of purified peptides are shown in Supporting Information Figure S1).

Peptide 5. ESI-MS (*m/z*): Calcd. for C₅₂H₈₀N₁₁O₂₀PS - H, 1240.4; Found, 1240.3 [M - H]⁻.

Peptide 6a. ESI-MS (*m/z*): Calcd. for C₅₁H₇₉N₁₂O₂₁PS + Na, 1281.5; Found, 1281.3 [M + Na]⁺.

Peptide 6b. ESI-MS (*m/z*): Calcd. for C₅₂H₈₃N₁₂O₁₉PS + H, 1243.5; Found, 1243.3 [M + H]⁺.

Peptide 6c. ESI-MS (*m/z*): Calcd. for C₅₃H₈₃N₁₂O₂₁PS + H, 1287.5; Found, 1287.4 [M + H]⁺.

Peptide 6d. ESI-MS (*m/z*): Calcd. for C₅₂H₈₃N₁₂O₁₉PS + Na, 1265.5; Found, 1265.4 [M + Na]⁺.

Peptide 6e. ESI-MS (*m/z*): Calcd. for C₅₉H₈₇N₁₂O₁₉PS + Na, 1251.5; Found, 1251.4 [M + Na]⁺.

Peptide 6f. ESI-MS (*m/z*): Calcd. for C₅₀H₇₇N₁₂O₂₁PS + Na, 1268.5; Found, 1268.2 [M + Na]⁺.

Synthesis of peptide 11a, 11b and 12. For peptides **11a**, **11b** and **12** active ester coupling was employed using N-Fmoc-protected amino acid (4 eq.), HATU (3.8 eq.), and DIEA (8.0 eq.) in N-methyl-2-pyrrolidinone (NMP). Coupling of Fmoc-L-Orn(Mtt)-OH was achieved using Fmoc-L-Orn(Mtt)-OH (2.0 eq.), HATU (1.9 eq.), and DIEA (4.0 eq.) in NMP by double coupling. After the completion of coupling of Fmoc-L-Orn(Mtt)-OH, the resin was then subjected to a global Mtt-deprotection by DCM/TFA/TIPS = 95:1:4 (10 min × 2). The resulting resins were washed with 10% DIEA in NMP and were subsequently coupled with 3,5-dichloroprridine-4-carboxylic acid or 4-(4-(trifluoromethyl)pridin-2-yl)benzoic acid (**10**). Peptide chains were then elongated using standard SPPS. The completed resins were treated with TFA/TIPS/H₂O cocktail (95:2.5:2.5) for 3 h and then filtered. Cold Et₂O was added to the filtrates and the resulting precipitates were washed with cold Et₂O (50 mL x 3). The crude

1
2
3 product was dissolved in DMSO and purified by reverse-phase preparative HPLC. (Analytical
4
5 HPLCs of purified peptides are shown in Supporting Information Figure S1).
6
7
8
9

10 **Peptide 11a.** Preparative HPLC conditions: linear gradient elution (79.9/20/0.1

11 H₂O/acetonitrile/TFA to 29.9/70/0.1 H₂O/acetonitrile/TFA over 30 minutes). ESI-MS (*m/z*)

12
13 Calcd. for C₆₆H₉₁F₃N₁₃O₁₉PS – H: 1488.6; Found [M – H][–] = 1488.4.
14
15

16 **Peptide 11b.** Preparative HPLC conditions: linear gradient elution (79.9/20/0.1

17 H₂O/acetonitrile/TFA to 54.9/45/0.1 H₂O/acetonitrile/TFA over 30 minutes). ESI-MS (*m/z*)

18
19 Calcd. for C₅₇H₈₀C₁₂N₁₃O₂₁PS – H: 1414.4; Found [M – H][–] = 1414.3.
20
21
22

23 **Peptide 12.** Preparative HPLC conditions: linear gradient elution (69.9/30/0.1

24 H₂O/acetonitrile/TFA to 39.9/60/0.1 H₂O/acetonitrile/TFA over 30 minutes). ESI-MS (*m/z*)

25
26 Calcd. for C₇₁H₉₁C₁₂F₃N₁₅O₂₀PS – H: 1662.5; Found [M – H][–] = 1662.3.
27
28
29
30
31
32

33 **Synthesis of peptides 13 – 15.** Peptides **13** – **15** were synthesized on Rink amide MBHA

34 resin by standard Fmoc solid-phase protocols using active ester coupling methodology as

35 described above, except that in *N*-methyl-2-pyrrolidone (NMP) was used in place of DMF.

36 Initial coupling was achieved on Fmoc-deprotected resin with a solution of Fmoc-L-

37 Orn(Mtt)-OH (5.0 eq.), HATU (5.0 eq.), HOAt (5.0 eq.), and DIEA (10 eq.) in NMP (5 mL).
38
39

40 The mixture was shaken for 3 h and the solvent was then drained. The resin was washed with

41 NMP (5 mL × 3, in 5 min/wash, drained after each wash) and *i*PrOH (5 mL × 3, in 5

42 min/wash, drained after each wash). The above sequence was repeated for the coupling of

43 Fmoc-L-Gly-OH (5.0 eq.) (for peptides **14** and **15**), Fmoc-L-Orn(Mtt)-OH (5.0 eq.), and

44 acetic anhydride in pyridine (1:9 v/v, 5 eq.). After the completion of peptide backbone, the

45 resin was then subjected to a global Mtt-deprotection in a wash sequence of 1% TFA in

46 CH₂Cl₂ (5 mL × 3, in 5 min/wash, drained after each wash), DIEA (5 mL × 3, in 5 min/wash,
47
48
49
50
51
52
53
54
55
56
57
58
59
60

1
2
3 drained after each wash), and NMP (5 mL × 3, in 5 min/wash, drained after each wash). The
4
5 resin was then reacted with a solution of 4-(4-(trifluoromethyl)pyridin-2-yl)benzoic acid (**10**,
6
7 10 eq.), HATU (5.0 eq.), HOAt (5.0 eq.), and DIEA (10 eq.) in NMP (5 mL). After shaking
8
9 (3 h), the solvent was drained. The resin was washed with NMP (5 mL × 3, in 5 min/wash,
10
11 drained after each wash) and *i*PrOH (5 mL × 3, in 5 min/wash, drained after each wash). The
12
13 final product was cleaved from the resin by shaking in a TFA/TIPS/H₂O cocktail (95:2.5:2.5)
14
15 (7.5 mL, 30 min). Another 7.5 mL portion of the cocktail was diluted with TFA (7.5 mL) to
16
17 make a 15 mL solution. This solution was used to wash the resin twice (7.5 mL/wash, in 15
18
19 min/wash). The filtrate was collected, combined and concentrated. Addition of cold Et₂O
20
21 caused precipitation of a white solid. The mixture was centrifuged and decanted. The white
22
23 precipitate was collected and washed with cold Et₂O (5 mL x 2). The crude product was
24
25 dissolved in CH₃CN and purified by reverse-phase preparative HPLC.

26
27
28
29
30 **Peptide 13** (Ac-OtOt-NH₂) 33 mg, 81% yield. ESI-MS (*m/z*) Calcd. for C₃₈H₃₇F₆N₇O₅,
31
32 785.3; Found [M + H]⁺ = 786.3, [M + Na]⁺ = 808.2, [M + 2H]⁺ = 393.7.

33
34
35 **Peptide 14** (Ac-OtGOt-NH₂): 26 mg, 59% yield. ESI-MS (*m/z*) Calcd. for C₄₀H₄₀F₆N₈O₆,
36
37 842.3; Found [M + H]⁺ = 843.3, [M + Na]⁺ = 865.3, [M + 2H]⁺ = 422.2.

38
39
40 **Peptide 15** (Ac-OtGGOt-NH₂): 16 mg, 34% yield. ESI-MS (*m/z*) Calcd. for C₄₂H₄₃F₆N₉O₇,
41
42 899.3; Found [M + H]⁺ = 900.2, [M + Na]⁺ = 922.2, [M + 2H]⁺ = 450.7.

43 44 45 46 47 48 **Biological**

49
50
51 **Materials.** Single pad and 16-pad nitrocellulose-coated FAST slides were purchased from
52
53 KeraFAST, Inc. (Boston, MA, USA). Gold SPRi slides and index matching oil were purchased
54
55 from Horiba Scientific (Edison, NJ, USA). NeutrAvidin, biotin-LC-NHS, biotin-PEG₁₂-NHS,
56
57 EDC, and NHS were purchased from Thermo Scientific (Rockford, IL, USA). Flexchip-

1
2
3 blocking buffer was purchased from GE Healthcare Life Sciences (Piscataway, NJ, USA). All
4
5 other reagents were purchased from Sigma-Aldrich (St. Louis, MO, USA) unless otherwise
6
7 mentioned.
8
9

10
11 **Proteins.** Monoclonal anti-pTyr mouse antibody was purchased from Cell Signaling
12
13 Technology, Inc. (#9411, Danvers, MA, USA). Alexafluor-conjugated goat anti-mouse
14
15 antibody was purchased from Life Technologies, Inc. (Grand Island, NY, USA). The PTPase
16
17 domain of YopH (residues 164–468) was expressed in *Escherichia coli* and purified as
18
19 described previously,³¹ as were the Variola major H1 (VH1)³² and human DUSP14 dual
20
21 specificity phosphatases.³³ The catalytic domain of human DUSP22 was expressed and
22
23 purified using methodology previously described.³⁴ The substrate trapping mutants of DUSP14
24
25 (C111S), DUSP22 (C88S), VH1 (C110S), and YopH (C403A/D356A) were constructed with
26
27 a QuikChange site-directed mutagenesis kit (Agilent Technologies), following the
28
29 manufacturer's instructions. The nucleotide sequences of all expression vectors were
30
31 confirmed experimentally.
32
33
34
35

36
37 **Generation of pTyr-peptide library arrays on nitrocellulose-substrates:** The aminoxy-
38
39 containing pTyr-peptides **6(a – f)**, oxime-containing pTyr-peptides, and **5** (100 μ M) were
40
41 mixed with NeutrAvidin (33 μ M) in citrate buffered saline (CBS; 10 mM citrate buffer and
42
43 100 mM NaCl, pH 6.2) containing 50% glycerol overnight at 4 °C. The NeutrAvidin-peptide
44
45 mixture was spotted identically onto 8 FAST-slide nitrocellulose slides in triplicate using an
46
47 inkjet ArrayJet microarrayer (Edinburgh, Scotland), and the slides were desiccated overnight
48
49 under vacuum (25 mm Hg) at 22 °C.
50
51
52
53

54
55 **Catalytic activity assay:** Protein concentrations were determined by UV/Vis using a
56
57 NanoDrop 2000 (Thermo Fischer Scientific, Waltham, MA, USA). Each slide was blocked
58
59
60

1
2
3 with 1x flexchip blocking buffer for 1 h at 22 °C. Individual slides were treated with a PTPase
4 diluted in CBS (pH 6.2) containing 0.05% Tween-20 and 1 mM DTT as follows: YopH (1
5 µg/mL, 1 min), VH1 (50 µg/mL, 15 min), DUSP14 (50 µg/mL, 15 min), and DUSP22 (100
6 µg/mL, 5 min). Two slides were treated with buffer only. Following the incubation periods,
7 the PTPase and buffer solutions were discarded and the slides were washed with 1x TBS-T (4
8 x 5mL, 3 min). The slides were then incubated with anti-pTyr mouse antibody (1:2000, 5 mL)
9 overnight at 4 °C followed by a wash step. The primary antibody was probed with an
10 Alexafluor647®-conjugated-conjugated goat anti-mouse antibody (1:2500, 5 mL) for 1 h at 22
11 °C. The slides were then washed with 1x TBS-T (4 x 5mL, 3 min) followed by one time with
12 distilled H₂O and then air dried. Each slide was scanned at 635 nm using a GenePix Microarray
13 Scanner 4400A (Molecular Devices, Sunnyvale, CA, USA) with the PMT Gain set to 400 and
14 the power setting at 10.
15
16
17
18
19
20
21
22
23
24
25
26
27
28
29
30

31 **Generation of pTyr-peptide subset arrays on Au-substrates:** Self-assembled monolayers
32 (SAMs) of 11-mercaptaundecanoic acid (11-MUA) were formed onto four gold slides by
33 submerging each clean slide in a 2.5 mM ethanolic solution of 11-MUA for 20 h at 22 °C and
34 rinsing with fresh EtOH. NeutrAvidin was then immobilized onto each surface via typical
35 amine-coupling chemistry: the slides were submerged in 5 mL of an aqueous mixture of EDC
36 (0.2M) and NHS (0.05 M) for 10 min at 22 °C, followed by 5 mL of NeutrAvidin (200 µg/mL)
37 in 10 mM sodium acetate (pH 5.0) for 2 h at 22 °C, and then 5 mL of 1 M ethanolamine-HCl
38 (pH 8.5) for 10 min at 22 °C. The slides were rinsed with distilled H₂O and then dried under a
39 gentle stream of nitrogen. The oxime-containing pTyr-peptides, **6(a – f)**, and **5** (100 µM in
40 CBS, pH 6.2, with 20% glycerol), as well as controls (biotin-LC-NHS and biotin-PEG₁₂ pre-
41 treated with 1M ethanolamine-HCl pH 8.5) were arrayed onto the NeutrAvidin-coated gold
42 slides in triplicate using an inkjet ArrayJet microarrayer, and the slides were desiccated
43
44
45
46
47
48
49
50
51
52
53
54
55
56
57
58
59
60

1
2
3 overnight under vacuum (25 Torr) at 22 °C. Spotted slides were stored at 4 °C in an air-tight
4
5 container before use.
6

7
8 **Kinetic assay:** The SPRi-Plex II (Horiba Scientific, Edison, NJ, USA) was cleaned and
9
10 calibrated before each experiment as per the manufacturer's instructions. Kinetic experiments
11
12 were performed at 25 °C in 1x CBS-P (pH 6.2) containing 1 mM DTT and 1x flexchip-blocking
13
14 buffer. Injections of anti-pTyr mAb (1 : 2000) were made before and after injection cycles of
15
16 PTPases to confirm reproducibility. Serially diluted catalytically inactive mutant PTPases
17
18 (DUSP14 C111S, DUSP22 C88S, VH1 C110S) were injected for 4 min at 50 μ L/min, followed
19
20 by 6 min of dissociation in buffer and then complete dissociation in 10 mM glycine-HCl pH
21
22 1.5 (2 min). PTPase concentrations were 0.05, 0.1, 0.5, 1, 2, and 5 μ M. Experiments were
23
24 repeated for DUSP22 C88S at concentrations of 0.1, 0.5, 1, 2.5, 5, 10, 20, and 40 μ M. YopH
25
26 C403A/D356A (1 μ M) and His₆-MBP (1 μ M) were also injected as positive and negative
27
28 controls, respectively. Sensorgrams were subtracted from reference spots and fitted to a
29
30 Langmuir binding curve using the ScrubberGen 2.0 software (Horiba Scientific, Edison, NJ,
31
32 USA).
33
34
35
36
37
38

39
40 **PTPase peptide substrate and inhibitor assays:** Oxime-functionalized pTyr-containing
41
42 peptides **6d-w33** and **6f-w202**, aminoxy-functionalized pTyr-containing peptides **6d** and **6f**,
43
44 and EGFR pTyr-containing peptides **5**, **11a**, **11b** and **12** (100 μ M each), were mixed with
45
46 NeutrAvidin (33 μ M) in CBS containing 40% glycerol for 30 min at 24 °C. Six replicates of
47
48 each NeutrAvidin-peptide mixture were spotted in 16 identical blocks on a 16-pad
49
50 nitrocellulose FAST slide using an ArrayJet microarrayer and the slide was desiccated
51
52 overnight under vacuum (25 mm Hg) at 22 °C. The slide was blocked with 1x flexchip blocking
53
54 buffer (5 mL) for 1 h at 22 °C. Using a 16-well gasket, each block was treated for 10 min with
55
56 25 μ g/mL (80 μ L) of either VH1, DUSP14, VH1(C110S), DUSP14(C111S) or 6 ng/mL of
57
58
59
60

1
2
3 either YopH or YopH (C403A/D356A), or buffer only. PTPase dilution buffer consisted of
4
5 CBS (pH 6.2) containing 0.05% Tween-20 and 1 mM DTT. The PTPase and buffer solutions
6
7 were discarded and the slides were washed with 1x TBS-T (3 x 5 mL, 5 min). The slides were
8
9 then incubated with anti-pTyr mouse antibody (1:1000, 5mL) for 1 h at 24 °C followed by a
10
11 wash step. The primary antibody was probed with an Alexafluor 647-conjugated goat anti-
12
13 mouse antibody (1 : 2500, 5 mL) for 1 h at 24 °C. The slides were then washed three times with
14
15 1x TBS-T followed by one time with distilled H₂O and then air dried. Each slide was scanned
16
17 at 635 nm using a GenePix Microarray Scanner 4400A (Molecular Devices, Sunnyvale, CA,
18
19 USA) with the PMT Gain set to 400 and the power setting at 10. The peptide **5** microarray,
20
21 assembled as above, was used to evaluate the inhibitory activity of fragment **w33** substituted
22
23 peptides **13**, **14**, and **15**. VH1 and DUSP14 were incubated (30 min, 24 °C) with dilutions (0 -
24
25 200µM) of **13-15**, and PTPase activity was assessed with the peptide **5** microarray (15 min, 24
26
27 °C) as above. IC₅₀ values for inhibitors were determined with peptide **5** concentrations of
28
29 178µM and inhibition curves that were fitted by nonlinear regression methods using ORIGIN
30
31 9.0 (OriginLab, Northampton, MA).
32
33
34
35
36
37
38
39
40

41 ASSOCIATED CONTENT

42
43 **Supporting information.** The structures of aldehydes used to make the oxime libraries,
44
45 analytical HPLCs of synthetic peptides, and additional Figures illustrating a heat map of
46
47 catalytic data and representative sensorgrams. This material is available free of charge via the
48
49 Internet at <http://pubs.acs.org>.
50
51
52
53

54 AUTHOR INFORMATION

55
56
57 **Corresponding Author:**
58
59
60

1
2
3 *Robert G. Ulrich; email: rulrich@bhsai.org; phone: (240) 446-8099
4

5 **Author Contributions**

6
7 MH, MB, TRB and RGU designed the experiments. MH, TRB, and RGU wrote the manuscript
8 with input from the coauthors. MH, MB, XZZ, JET, BMZ, TXN, KT and SC performed
9 experiments. MH, MB, RGU, TRB, GTL, BMZ, and DSW analyzed the data.
10
11
12
13

14 **Notes**

15
16 The content of this publication does not necessarily reflect the views or policies of the
17 Department of Health and Human Services or the Department of Defense, nor does the mention
18 of trade names, commercial products or organizations imply endorsement by the U.S.
19 Government. The authors declare no competing financial interest.
20
21
22
23
24
25
26
27

28 **ACKNOWLEDGEMENTS**

29
30
31 This project was supported in part by federal funds from the Frederick National Laboratory for
32 Cancer Research, National Institutes of Health, under contract HHSN261200800001E and the
33 Intramural Research Program of the NIH, National Cancer Institute, Center for Cancer
34 Research, and by appointment of MH and BMZ to the Research Participation Program for the
35 U.S. Army Medical Research and Materiel Command, administered through an agreement
36 between the U.S. Department of Energy and the USAMRMC. This work was supported in part
37 by a JSPS Research Fellowship for Japanese Biomedical and Behavioral Researchers at NIH
38 (KT).
39
40
41
42
43
44
45
46
47
48
49
50
51
52

53 **ABBREVIATIONS USED**

54
55
56
57
58
59
60

1
2
3 DUSP, dual-specificity phosphatase; pTyr, phosphotyrosine; PTPase, protein tyrosine
4 phosphatase; SPR, surface plasmon resonance; VH1, Variola major H1; YopH, *Yersinia* outer
5
6 protein H
7
8
9
10
11

12 REFERENCES

- 13
14
15 1. Alonso, A.; Sasin, J.; Bottini, N.; Friedberg, I.; Osterman, A.; Godzik, A.; Hunter, T.;
16 Dixon, J.; Mustelin, T., Protein Tyrosine Phosphatases in the Human Genome. *Cell* **2004**, *117*
17 (6), 699-711.
18
19
20
21 2. Tonks, N. K., Protein tyrosine phosphatases - from housekeeping enzymes to master
22 regulators of signal transduction. *FEBS J.* **2012**, *280* (2), 346-378.
23
24
25 3. Tautz, L.; Mustelin, T., Strategies for developing protein tyrosine phosphatase
26 inhibitors. *Methods* **2007**, *42*, 250-260.
27
28
29 4. Gao, Y.; Wu, L.; Luo, J. H.; Yang, D.; Zhang, Z.-Y.; Burke, T. R., Jr., Examination of
30 novel non-phosphorous-containing phosphotyrosyl mimetics against Protein Tyrosine
31 Phosphatase 1B and demonstration of differential affinities toward Grb2 SH2 domains.
32 *Bioorg. Med. Chem. Lett.* **2000**, *10*, 923-927.
33
34
35 5. Wood, W. J.; Patterson, A. W.; Tsuruoka, H.; Jain, R. K.; Ellman, J. A., Substrate
36 activity screening: a fragment-based method for the rapid identification of nonpeptidic
37 protease inhibitors. *J. Am. Chem. Soc.* **2005**, *127* (44), 15521-7.
38
39
40 6. Erlanson, D. A.; Wells, J. A.; Braisted, A. C., Tethering: Fragment-Based Drug
41 Discovery. *Annu. Rev. Biophys. Biomol. Struct.* **2004**, *33*, 199-223.
42
43
44 7. Vetter, S. W.; Keng, Y.-F.; Lawrence, D. S.; Zhang, Z.-Y., Assessment of Protein-
45 tyrosine Phosphatase 1B substrate specificity using "Inverse Alanine Screening". *J. Biol.*
46 *Chem.* **2000**, *275*, 2265-2268.
47
48
49
50
51
52
53
54
55
56
57
58
59
60

- 1
2
3 8. Köhn, M.; Gutierrez-Rodrguez, M.; Jonkheijm, P.; Wetzel, S.; Wacker, R.; Schroeder,
4 H.; Prinz, H.; Niemeyer, C. M.; Breinbauer, R.; Szedlaczek, S. E.; Waldmann, H., A
5
6 microarray strategy for mapping the substrate specificity of protein tyrosine phosphatases.
7
8 *Angew. Chem. Int. Ed.* **2007**, *46*, 7700-7703.
9
10
11
12 9. Mitra, S.; Barrios, A. M., Identifying selective protein tyrosine phosphatase substrates
13 and inhibitors from a fluorogenic, combinatorial peptide library. *ChemBioChem* **2008**, *9*,
14
15 1216-1219.
16
17
18 10. Rotin, D.; Margolis, B.; Mohammadi, M.; Daly, R. J.; Daum, G.; Li, N.; Fischer, E. H.;
19 Burgess, W. H.; Ullrich, A.; Schlessinger, J., SH2 domains prevent tyrosine
20
21 dephosphorylation of the EGF receptor: identification of Try992 as the high-affinity binding
22
23 site for SH2 domains of phospholipase C gamma. *EMBO J.* **1992**, *11* (2), 559-567.
24
25
26 11. Beresford, N.; Patel, S.; Armstrong, J.; Balázs, S.; Fordham-Skelton, A. P.; Taberero,
27 L., MptpB, a virulence factor from Mycobacterium tuberculosis, exhibits triple-specificity
28
29 phosphatase activity. *Biochem. J.* **2007**, *406*, 13-18.
30
31
32 12. Zhang, Z.-Y.; Maclean, D.; McNamara, D. J.; Sawyer, T. K.; Dixon, J. E., Protein
33
34 tyrosine phosphatase substrate specificity: size and phosphotyrosine position requirements in
35
36 peptide substrates. *Biochemistry* **1994**, *33*, 2285-2290.
37
38
39 13. Flint, A. J.; Tiganis, T.; Barford, D.; Tonks, N. K., Development of "substrate-trapping"
40
41 mutants to identify physiological substrates of protein tyrosine phosphatases. *Proc. Natl.*
42
43 *Acad. Sci. USA* **1997**, *94*, 1680-1685.
44
45
46 14. Blanchetot, C.; Chagnon, M.; Dubé, N.; Hallé, M.; Tremblay, M. L., Substrate-trapping
47
48 techniques in the identification of cellular PTP targets. *Methods* **2005**, *35* (1), 44-53.
49
50
51 15. Ivanov, M.; Stuckey, J. A.; Schubert, H. L.; Saper, M. A.; Bliska, J. B., Two substrate-
52
53 targeting sites in the Yersinia protein tyrosine phosphatase co-operate to promote bacterial
54
55 virulence. *Mol. Microbiol.* **2005**, *55* (5), 1346-1356.
56
57
58
59
60

- 1
2
3
4
5
6
7
8
9
10
11
12
13
14
15
16
17
18
19
20
21
22
23
24
25
26
27
28
29
30
31
32
33
34
35
36
37
38
39
40
41
42
43
44
45
46
47
48
49
50
51
52
53
54
55
56
57
58
59
60
16. Haney, C. M.; Loch, M. T.; Horne, W. S., Promoting peptide α -helix formation with dynamic covalent oxime side-chain cross-links. *Chem. Commun.* **2011**, *47*, 10915-10917.
17. Liu, F.; Thomas, J.; Burke, T. R., Jr., Synthesis of homologous series of sidechain-extended orthogonally protected aminooxy-containing amino acids. *Synthesis* **2008**, 2432-2438.
18. Liu, F.; Stephen, A. G.; Waheed, A. A.; Aman, M. J.; Freed, E. O.; Fisher, R. J.; Burke, T. R., Jr., SAR by oxime-containing peptide libraries: application to Tsg101 ligand optimization. *ChemBioChem* **2008**, *9*, 2000-2004.
19. Shao, J.; Tam, J. P., Unprotected Peptides as Building Blocks for the Synthesis of Peptide Dendrimers with Oxime, Hydrazone, and Thiazolidine Linkages. *Journal of the American Chemical Society* **1995**, *117* (14), 3893-3899.
20. Rose, K.; Zeng, W.; Regamey, P.-O.; Chernushevich, I. V.; Standing, K. G.; Gaertner, H. F., Natural Peptides as Building Blocks for the Synthesis of Large Protein-like Molecules with Hydrazone and Oxime Linkages. *Bioconjugate Chemistry* **1996**, *7* (5), 552-556.
21. Kalia, J.; Raines, R. T., Hydrolytic stability of hydrazones and oximes. *Angew Chem Int Ed Engl* **2008**, *47* (39), 7523-6.
22. Liu, F.; Stephen, A. G.; Waheed, A. A.; Aman, M. J.; Freed, E. O.; Fisher, R. J.; Burke, T. R., Jr., SAR by oxime-containing peptide libraries: application to Tsg101 ligand optimization. *Chembiochem : a European journal of chemical biology* **2008**, *9* (12), 2000-2004.
23. Liu, F.; Park, J.-E.; Qian, W.-J.; Lim, D.; Scharow, A.; Berg, T.; Yaffe, M. B.; Lee, K. S.; Burke, T. R., Identification of High Affinity Polo-like Kinase 1 (Plk1) Polo-box Domain Binding Peptides Using Oxime-Based Diversification. *ACS Chemical Biology* **2012**, *7* (5), 805-810.

- 1
2
3 24. Bahta, M.; Liu, F.; Kim, S.-E.; Stephen, A. G.; Fisher, R. J.; Burke Jr, T. R., Oxime-
4 based linker libraries as a general approach for the rapid generation and screening of
5
6 multidentate inhibitors. *Nature Protocols* **2012**, *7*, 686.
7
8
9
10 25. Zhao, X. Z.; Hymel, D.; R. Burke, T., *Application of oxime-diversification to optimize*
11
12 *ligand interactions within a cryptic pocket of the polo-like kinase 1 polo-box domain*. 2016;
13
14 Vol. 26.
15
16
17 26. Stillman, B. A.; Tonkinson, J. L., FAST slides: a novel surface for microarrays.
18
19 *Biotechniques* **2000**, *29* (3), 630-5.
20
21
22 27. de la Puerta, M. L.; Trinidad, A. G.; Rodríguez, M.; Bogetz, J.; Sánchez Crespo, M.;
23
24 Mustelin, T.; Alonso, A.; Bayón, Y., Characterization of new substrates targeted by *Yersinia*
25
26 tyrosine phosphatase YopH. *PLOS ONE* **2009**, *4* (2), e4431.
27
28
29 28. Zhang, Z.-Y.; Thieme-Seffler, A. M.; Maclean, D.; McNamara, D. J.; Dobrusin, E. M.;
30
31 Sawyer, T. K.; Dixon, J. E., Substrate specificity of the protein tyrosine phosphatases. *Proc.*
32
33 *Natl. Acad. Sci. USA* **1993**, *90*, 4446-4450.
34
35
36 29. Zhang, S.; Chen, L.; Luo, Y.; Gunawan, A.; Lawrence, D.S.; Zhang, Z.-Y., Acquisition
37
38 of a potent and selective TC-PTP inhibitor via a stepwise fluorophore-tagged combinatorial
39
40 synthesis and screening strategy. *J. Am. Chem. Soc.* **2009**, *131*, 13072-13079.
41
42
43 30. Zhang, S.; Liu, S.; Tao, R.; Wei, D.; Chen, L.; Shen, W.; Yu, Z.H.; Wang, L.; Jones,
44
45 D.R.; Dong, X.C.; Zhang, Z.-Y. A highly selective and potent PTP-MEG2 inhibitor with
46
47 therapeutic potential for type 2 diabetes. *J. Am. Chem. Soc.* **2012**, *134*, 18116-18124.
48
49
50 31. Zhang, Z.-Y.; Clemens, J. C.; Schubert, H. L.; Stuckey, J. A.; Fischer, M. W.; Hume, D.
51
52 M.; Saper, M. A.; Dixon, J. E., Expression, purification, and physicochemical characterisation
53
54 of a recombinant *Yersinia* protein tyrosine phosphatase. *J. Biol. Chem.* **1992**, *267*, 23759-
55
56 23766.
57
58
59
60

- 1
2
3 32. Tropea, J. E.; Phan, J.; Waugh, D. S., Overproduction, purification, and biochemical
4 characterisation of the dual specificity H1 protein phosphatase encoded by Variola Major
5
6
7
8 Virus. *Protein Expression and Purification* **2006**, *50*, 31-36.
9
- 10 33. Lountos, G. T.; Tropea, J. E.; Cherry, S.; Waugh, D. S., Overproduction, purification,
11 and structure determination of human dual specificity phosphatase 14. *Acta*
12
13
14 *Crystallographica Section D* **2009**, *65*, 1013-1020.
15
- 16 34. Tropea, J. E.; Cherry, S.; Nallamsetty, S.; Bignon, C.; Waugh, D. S., *A generic method*
17
18
19 *for the production of recombinant proteins in Escherichia coli using a dual hexahistidine-*
20
21
22 *maltose-binding protein affinity*. Humana Press, Inc.: Totowa, NJ, 2007.
23
24
25
26
27
28
29
30
31
32
33
34
35
36
37
38
39
40
41
42
43
44
45
46
47
48
49
50
51
52
53
54
55
56
57
58
59
60